CDF/PUB/TRACKING/PUBLIC/5306

4 May 2000

Characteristics of Hamamatsu ISL Class B Sensors

K. Hara [a] S. Kim [a] M. Shimojima [a] H. Suzuki [a] K. Takikawa [a]
Y. Taniguchi [a] J. Goldstein [b] J. Incandela [b] D. Stuart [b]
G. Grim [c] C. Hill [c]

[a] *University of Tsukuba, Institute of Physics, Tsukuba, Ibaraki 305-8571, Japan*

[b] *Fermilab, P.O. Box 500, Batavia IL 60513, USA*

[c] *UC Davis, Department of Physics, Davis, CA 95616, USA*

Abstract

The production of ISL Hamamatsu sensors has completed in January 2000. Among the total delivery of 494 sensors, there are 92 sensors of which leakage current requirements are slightly loosened from the original specifications. We have investigated the electrical characterisitics of these sensors, called Class B, and accepted them as the delivery. This note summarizes those measurements already reported in CDFnote 4893 and extended measurements which include the radiation damage study with protons and a long-term stability test. ISL sensors will receive about 5×10^{12} protons/cm^2 (or 0.15 Mrad) at r=20 cm after a collection of data corresponding to 30 fb^{-1}. We have examined the electrical performances of Class A and B sensors which were irradiated with ^{60}Co γ's to 0.2 Mrad and with 63-MeV protons to the fluence of (2–8)$\times 10^{12}$ cm^{-2}. The results and stability tests show that there will be no unexpected degradation in the performance of Class B sensors.

Key words: silicon microstrip detector; radiation damage; long-term stability; micro-discharge

1 Introduction

The silicon microstrip sensor of the ISL detector[1] is AC-coupled and double sided with the electrode strips forming a small stereo angle of $\sim 1.2^\circ$. The strip pitch is 112 μm and the number of readout strips is 512 per plane for both sides. Such Si sensors are arranged into ladders, each consisting of six Si

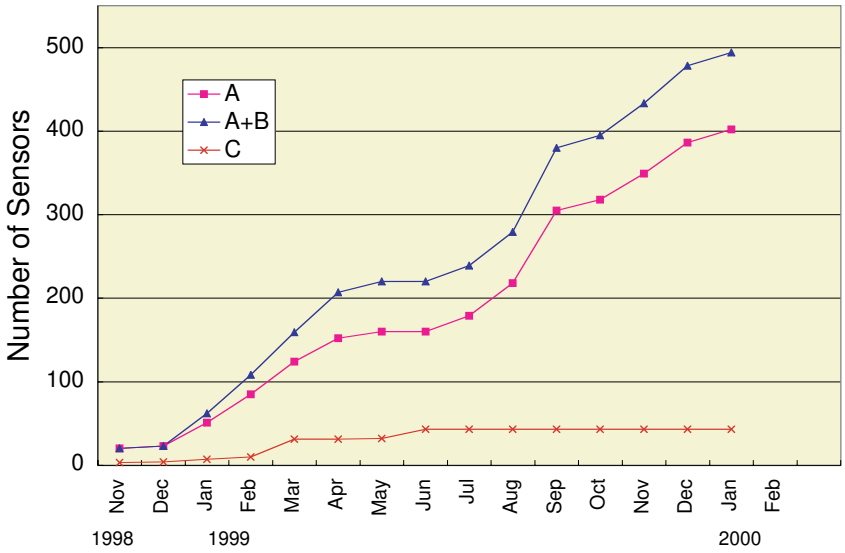

Fig. 1. The delivery history of Hamamatsu ISL sensors. A+B are used for real detector production while C are electrical and mechanical testing.

microstrip sensors lined along the beam direction. The ladders are arranged into one central barrel (r=22 cm) and two endplug barrels (r=20 and 28 cm) on each end.

The ISL sensors for the inner-radius three barrels were fabricated by Hamamatsu Photonics Co. (HPK) using 4" technology [2],[3]. The sensitive area of the sensor is 57.2 mm wide and 67.5 mm long with the thickness of 300 μm. The total number of sensors required is 456. In January 2000 HPK has completed the production of 494 sensors [1] . Since the delivery started in November 1998, the whole production took about twice the original estimate of 8 months. The delivery history is plotted in Fig. 1. One of the reasons for this delay was due to the delay of the whole project - HPK sensor production was never the critical part in the project and HPK intruded some other commercial production in summer 1999. Another reason was that the rejection fraction was greater than expected due to I-V characteristics and to p-side dead channels.

In order to partially recover the yield, we have slightly loosened the requirement on the leakage current[2]. The degraded I-V characteristics of Class B sensors is represented by that of a few strips which draw large leakage currents. These are most probably micro-discharges which are created in large electrical field caused by some defects made during the process. For Class B sensors we counted the channel is dead if the leakage current through that channel exceeds 200 nA at 140 V.

Once the detector is proven to be usable from the initial evaluation, the long-

[1] The final delivery took place in March waiting for qualification of the delivered sensors.

term stability has to be verified. The long-term stability hereby includes the stability against the radiation.

Since the ISL sensors are located outside the SVX-II detectors, the radiation environment is modest. According to [4] and extrapolating the radiation level at r=20 cm, ISL sensors are expected[2] to receive 5×10^{12} protons/cm^2 or 0.15 Mrad after a collection of data corresponding to 30 fb^{-1}.

In this note, we report the characterization of Class B sensors with emphasis on long-term stability and radiation hardness. The radiation hardness was evaluated both for ^{60}Co γ's and 63-MeV protons.

2 Initial characteristics of Class B sensors

Fig. 2 shows the distributions of the total leakage current for all the delivered sensors measured at 100 V and at 130 V, and of the leakage current increase ΔI between the two voltages.

Although most of the sensors populate in the region $\Delta I < 0.3$ μA, there is a long tail in the larger ΔI region. We define Class B to satisfy $0.3 < \Delta I < 1$ μA. We note that Class B sensors tend to show larger leakage current both at 100 V and 130 V.

In Fig. 3 plotted is the total leakage current of Sensor No. 3 against the bias voltage, Sensor No. 3 being an example of Class B. Also shown in the figure are some of the individual strip current measured by probing the DC pads connected to the implant strips. Since the strip leakage currents are read out from the ohmic side, the measured strip leakage current is of the particular single strip above the fully depletion voltage, *i.e.* $V >\sim 80$ V. This sensor has only two leaky strips, strip #008 and #009. These two contribute entirely to the large increase in the total current. The rest of the strips including the very neighbors show a plateau up to 200 V we measured.

We have required that the strip leakage current of Class B sensors be less than 200 nA at 140 V bais voltage, otherwise the channel is counted as dead. Fig. 4 shows the distribution of numbers of such strips measured on p side. At HPK, the strip leakage current of Class B sensors was measured on p side only with biasing through a dedicated n^+ electrode implanted along the sides on p side. For the n side, which requires wirebonding for biasing, the strip leakage

[2] The proton fluence is calculated using $\Phi(2\ \mathrm{fb}^{-1}) = \frac{6.68 \times 10^{13}}{r^{1.7}}$ cm^{-2} (r, radial distance from the interaction point is in cm), where the contributions of loopers and secondary interactions are effectively taken into account. The radiation absorption dose of 300 μm thick silicon is given by 1 Mrad = 3.8 $\times 10^{13}$ mips/cm^2.

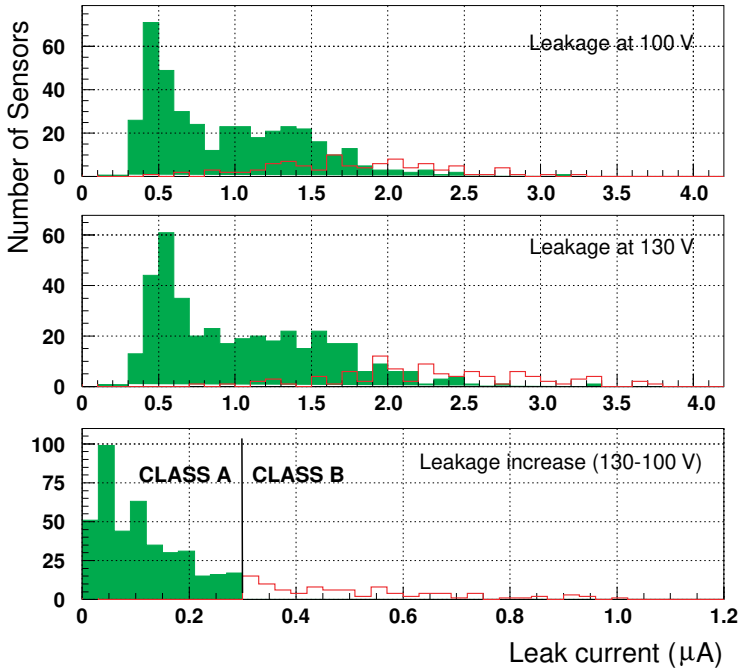

Fig. 2. Distributions of the leakage currents at V=100 and 130 V, and of their difference.

current was not measured at HPK. Instead, we assumed that the number of leaky strips on n side is same as that on p side: Large current is induced similarly on both sides at the strips where the micro-discharge is occuring. This assumption is also verified to be roughly correct from measurements on several samples.

The requirement of <200 nA is arbitrary since the amplifier noise is not affected by the leakage current of that level. In fact, we grouped Class B sensors to be used in the same half-ladders, where those leaky strips were also wire-bonded. There are so far nine half-ladders which are constructed using Class B sensors only. We investigated the possible correlation between the noise level and the leakage current summed over the three strips which make up a readout channel. The correlation is shown in Fig. 5. Shown are only the data points where the channel leakage is more than 100 nA or the measured noise level is more than ∼3.5 ADC counts. The noise value is truncated at 5 ADC counts in this plot. We note that the noise level of genuine channels is typical 3 ADC counts. There are several channels with noise value more than 4 ADC counts, but there seems no strong correlation with the channel leakage current up to ∼1000 nA we investigated. The noise in the figure was measured right after the half-ladders are constructed, which tends to decrease through the burn-in process.

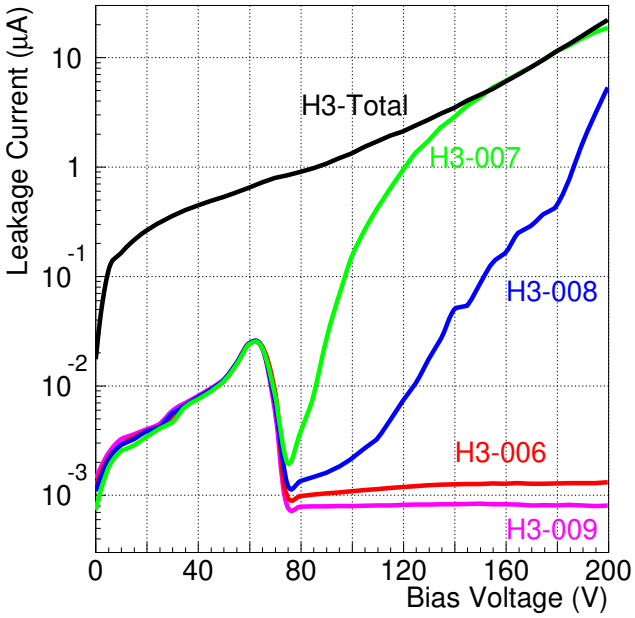

Fig. 3. Total leakage current and some of the n-side strip leakage currents as a function of bias voltage. The strips not shown in the plot behave similar to Strips 6 and 9.

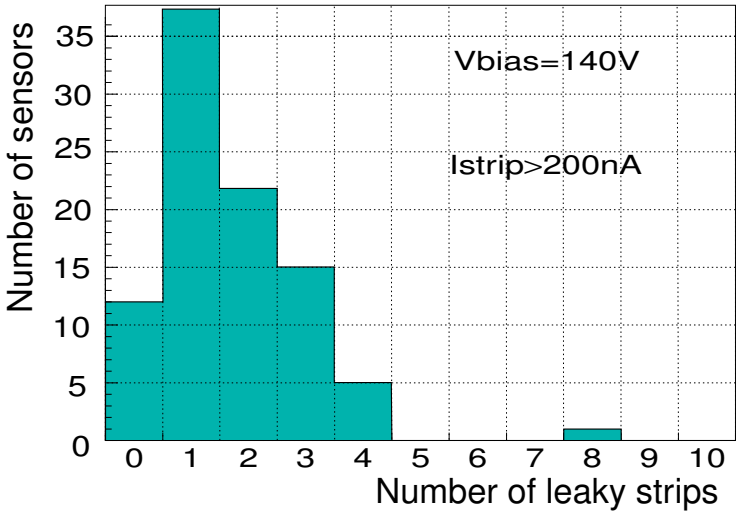

Fig. 4. Number of strips with >200 nA leakage current.

3 Long-term stability

The sensors have shown to function electrically with negligible increase in the noise even for the strips with $\sim$1 μA leakage current. In order to study the possible instabilty of such sensors, we have carried out a long-term stability test. A total of seven sensors were kept biased for 90 days in a thermostat chamber

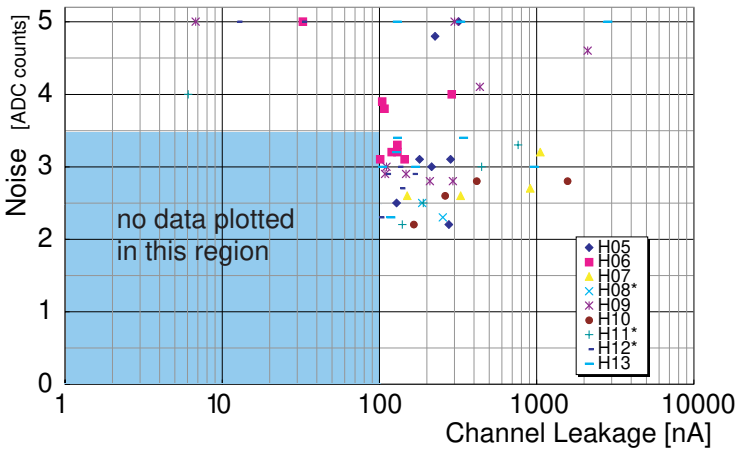

Fig. 5. Correlation between the half-ladder noise levels and the strip leakage currents.

where the temperature was controlled to 20°C. The measured humidity ranged from 15 to 20%.

Seven sensors were selected for their varying I-V characteristics: three Class A (199, 200, 201), two Class B (195, 202) and even worse (Class C) sensors (203 and 204) (See Fig. 6).

While keeping the bias voltage at 120 V, the leakage currents of seven sensors were monitored by measuring the voltage drops across 100 kΩ resistors which were placed serially in the bias lines. In order to measure the stability at a higher voltage, the leakage current was measured also at 150 V: the bias voltage was raised to 150 V only during this measurement. The stability of

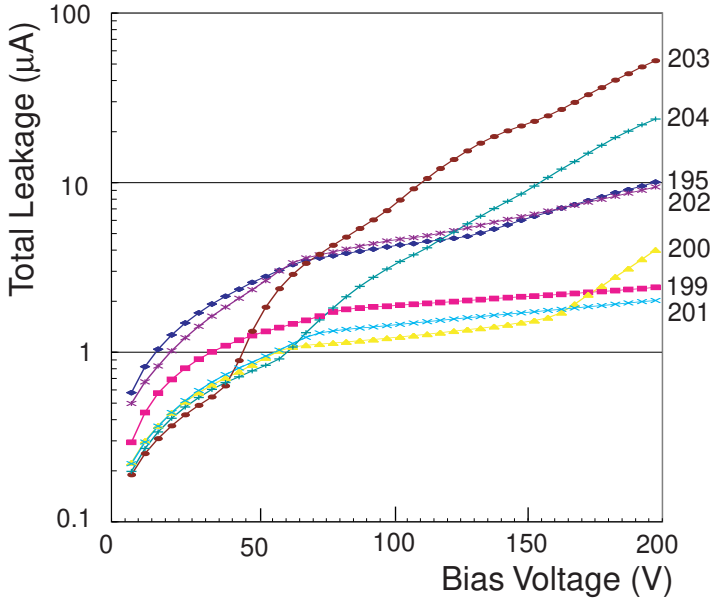

Fig. 6. The initial I-V curves of sensors used for the long-term stability test.

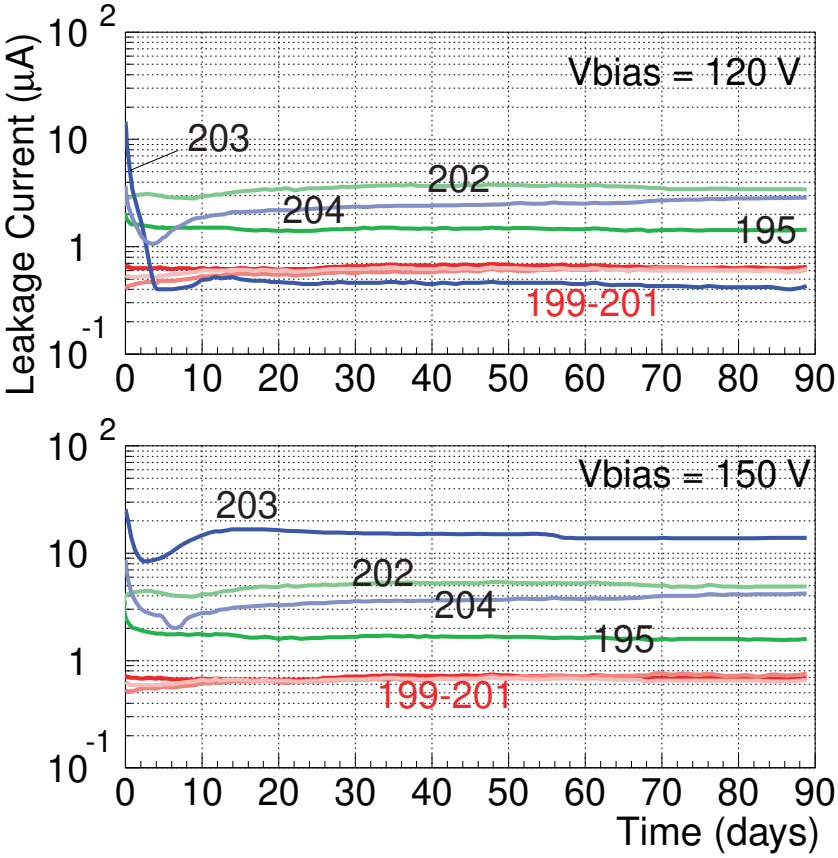

Fig. 7. Stability of leakage measured at 120 V and 150 V.

the leakage current is plotted in Fig. 7. We note changes for the two Class C sensors in the first ten days but the leakage current thereafter and for Class A and B sensors are stable.

The I-V characteristics were measured on day 5, day 65 and day 88. On day 5, Class C sensors (203 and 204), after showing a large decrease in the leakage current as shown in Fig. 7, showed a plateau above the full depletion voltage, which then could be categorized as Class B. Since day 5, the I-V curves of these two sensors were stable but showed a small shift in the onset voltage of micro-discharge of the order of 5–10 V. The I-V curves of other sensors were quite stable throughout the test.

This long-term stability test can be summarized that Class A and B are stable from the very beginning and that sensors with even large ΔI (Class C) can also be stabilized to some level within 5–10 days.

4 Stabilty against radiation

4.1 ^{60}Co-γ irradiation

Three sensors were first irradiated with ^{60}Co γ's at Japan Atomic Energy Research Institute, Tokai. The samples were placed in a irradiation cave at a fixed distance of 50 cm and were irradiated uniformly to 0.2 Mrad at a rate of 30 krad/h.

Since the global features of HPK microstrip sensors against ^{60}Co-γ's have been reported elsewhere[5], we concentrated on the measurement of strip leakage current distribution in order to evaluate the possible influence from the leaky channels.

The post irradiation measurements were made 2–4 days after the irradiation. From the previous experience[5] the sensors are still underway of annealing but should have experienced the major part of the annealing. In fact the total leakage current measured 2–4 days after decreased only by $\sim$20% compared to that measured 4 h after the irradiation.

4.2 Proton irradiation

The proton irradiation was made at the UC Davis 63-MeV Proton Cyclotron. The beam profile was approximately uniform over a 7 cm diameter. The three samples already irradiated with ^{60}Co γ's were irradiated with protons to fluences of 2, 4 and 8×10^{12} cm^{-2}. The irradiation was made at room temperature without biasing to the sensors. The sensors were kept refregirated after the irradiation and shipped to Japan in a dry-ice box. The characterization of the samples was made at room temperature at Univ. of Tsukuba. Note that the 63-MeV proton fluence of 8×10^{12} cm^{-2} adds additional ionizing dose of about 0.4 Mrad. The NIEL, non-ionizing energy loss, of 63-MeV protons is about 2 times that of 1-MeV neutrons[6]. Hereafter the three proton fluences are scaled to 4, 8 and 16×10^{12} cm^{-2} by translating in 1-MeV neutron equivalent fluence.

4.3 I-V characteristics

In Fig. 8, the *I-V* curves of the three sensors are shown. We have selected these sensors for varying *I-V* characteristics: No. 196 is Class A; No. 197 has one very leaky strip and shows a micro-discharge onset at $\sim$75 V (Class C);

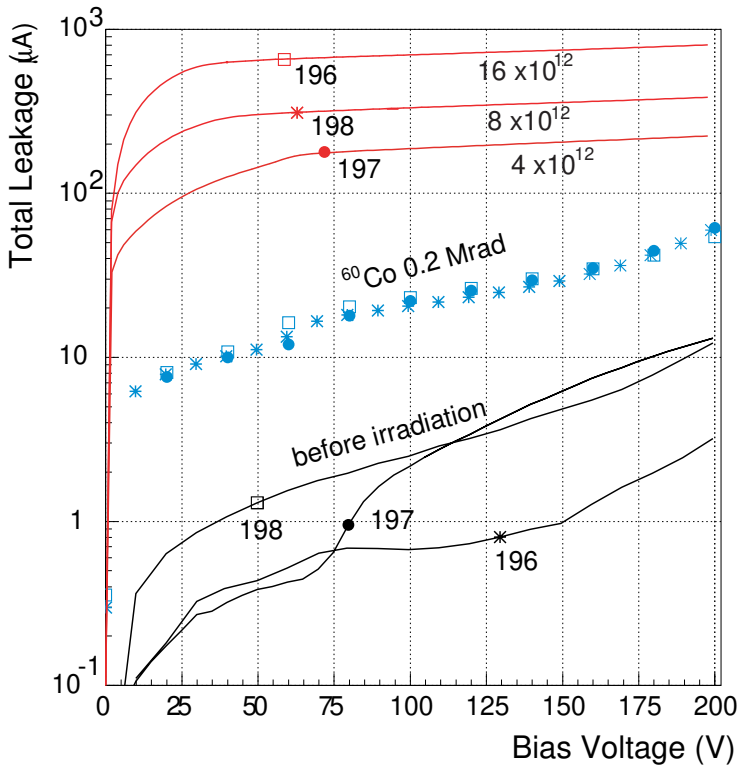

Fig. 8. I-V curves of three sensors, measured before, 3 days after 0.2 Mrad irradiation with γ's, and 4 months after neutron equivalent fluence of (4–18) $\times$ 10^{12} cm^{-2}.

and No. 198 has some clusters of leaky strips (Class B but on the boundary to Class C).

Although the initial I-V characteristics are different, they are identical after the irradiation with 0.2 Mrad γ's. Effects of surface charge accumulation through the γ irradiation dominate over the individual difference observed at pre-irradiation.

The increase of leakage current due to proton irradiation is attributed to creation of defects in the bulk silicon. This effect is characterized by the damage constant which is defined as the ratio of the leakage current increase per detector volume to the irradiation fluence. Fig. 9 shows the total leakage current measured at the full depletion voltage as a function of the fluence. The measured leakage current is translated to that at 20°C, since the measurement was made at 25°C. The three data points lie on a straight line, from which we extract the damage constant to be (3.9 $\pm$ 0.6) $\times$ 10^{-17} A/cm. The error is entirely due to the uncertainty in the translation factor from NIEL of 63-MeV protons to that of 1-MeV neutrons. The obtained damage constant is consistent with previous measurements $e.g.$ reported in [6].

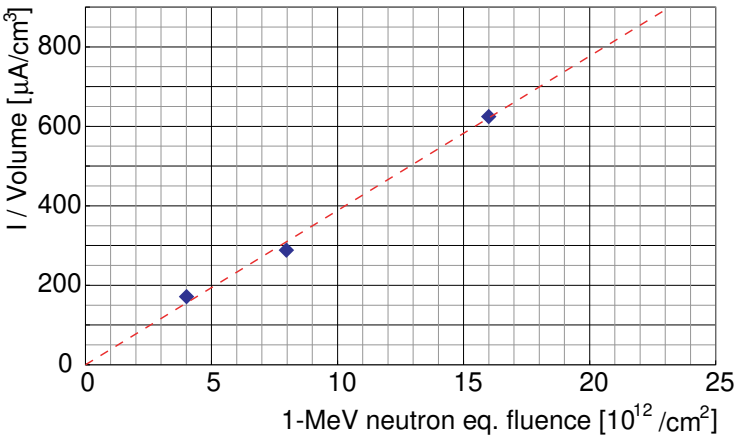

Fig. 9. The increase of leakage current normalized by volume as a function of neutron equivalent fluence.

4.4 Individual strip leakage current

Figs 10, 11 and 12 show the strip leakage currents measured at 140 V before and after γ and proton irradiations. The average strip leakage current was at the 1 nA level before irradiation, which increased to $\sim$50 nA after 0.2 Mrad γ irradiation. The strip current after the proton irradiation is less than 2 μA depending on the proton fluence.

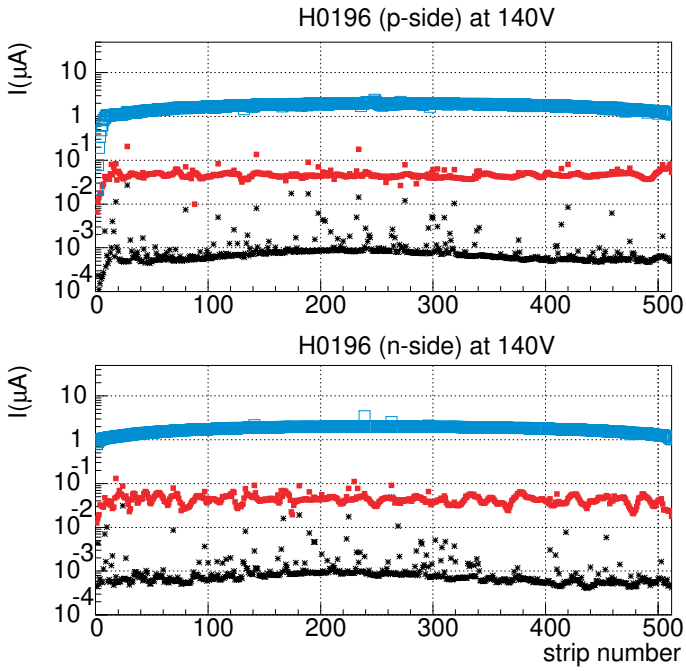

Fig. 10. Strip leakage current of No. 196 sensor (Class A) before (crosses), after (circles) ^{60}Co-γ, and after (squares) 16 $\times$ 10^{12} cm^{-2} neutron equivalent fluence. (Top) p-side and (above) n-side.

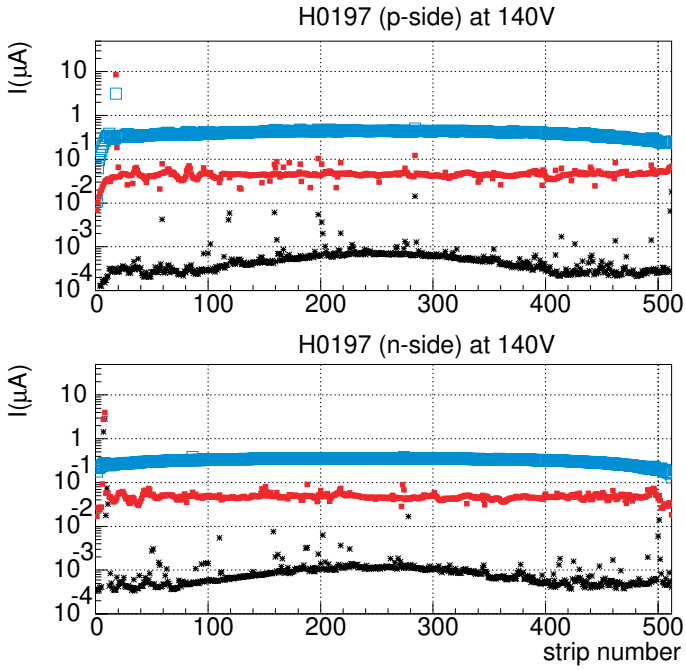

Fig. 11. Strip leakage current of No. 197 sensor (Class C) before (crosses), after (circles) ^{60}Co-γ, and after (squares) 4×10^{12} cm^{-2} neutron equivalent fluence. (Top) p-side and (above) n-side.

Sensor 197 showed a few leaky strips in 5–10 channels only on n side before irradiation. The corresponding p side strips started to show also large leakage after the γ and proton irradiations. The rest of the strips are not influenced from these leaky strips. Sensor 198 showed some clusters of leaky strips before irradiation. Although these clusters are still recognizable after the γ irradiation, the enhancement becomes smaller after the proton irradiation. The effects of leaky strips tend to diminish as the average strip leakage current increases by irradiation.

4.5 Full depletion voltage

The full depletion voltage decreases initially with proton radiation since the radiation-induced defects act as donors and the initial acceptor impurities are partially cancelled with defects. Above the certain radiation level, the initial n type bulk is inverted into p type bulk.

Fig. 13 shows the full depletion voltages determined from C-V curves. The full depletion voltage before the irradiation ranged from 70 to 90 V. In order to compare with a prediction, the data are plotted after normalizing such that the initial full depletion voltage is 80 V. The overlaied curves are predictions

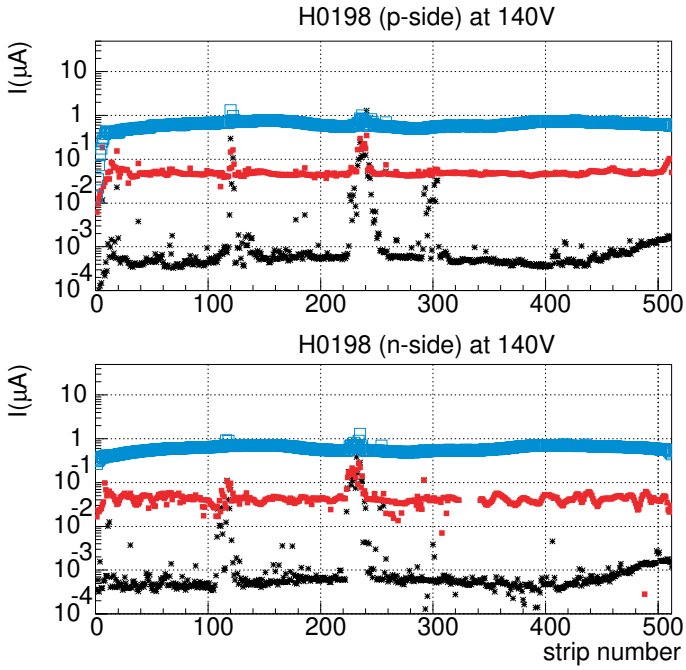

Fig. 12. Strip leakage current of No. 198 sensor (Class B) before (crosses), after (circles) ^{60}Co-γ, and after (squares) 8×10^{12} cm^{-2} neutron equivalent fluence. (Top) p-side and (above) n-side.

calculated using parameter sets [3] given in [7]:

$$\mathrm{N_{eff}}(\Phi)=\mathrm{N_{eff}}(0)-\mathrm{N_D}\{1-\exp(-c\Phi)\}-(g_c+g_Y)\Phi$$

where Φ is the fluence and we assumed that the initial acceptors are fully removed (R=$\mathrm{N_D}/\mathrm{N_{eff}}(0)$=1) or a half of them are removed (R=0.5) due to proton irradiation. Under a planer diode assumption of 300 μm thickness, the effective impurity density $\mathrm{N_{eff}}$ is related to the full depletion voltage $\mathrm{V_{dep}}$ through the relation:

$$\mathrm{N_{eff}}=1.46\times10^{10}\ \mathrm{V_{dep}}\ \mathrm{cm^{-3}V^{-1}},$$

which fixes the parameter $\mathrm{N_{eff}}(0)$ to reproduce the initial full depletion voltage of 80 V. Our data agree better to the curve with R $\sim$0.5. The fluence we expect after 30 fb^{-1} is indicated in the figure. Throughout the lifetime of the ISL sensors, the full depletion voltage will be in the range of monotonical decrease.

[3] $g_Y = 5.8\times10^{-2}$ cm^{-1}, $g_c = 1.15\times10^{-2}$ cm^{-1}, $c = 0.96\times10^{-13}$ cm^2. The time dependent term k is neglected since the measurement was made sufficiently after the irradiation.

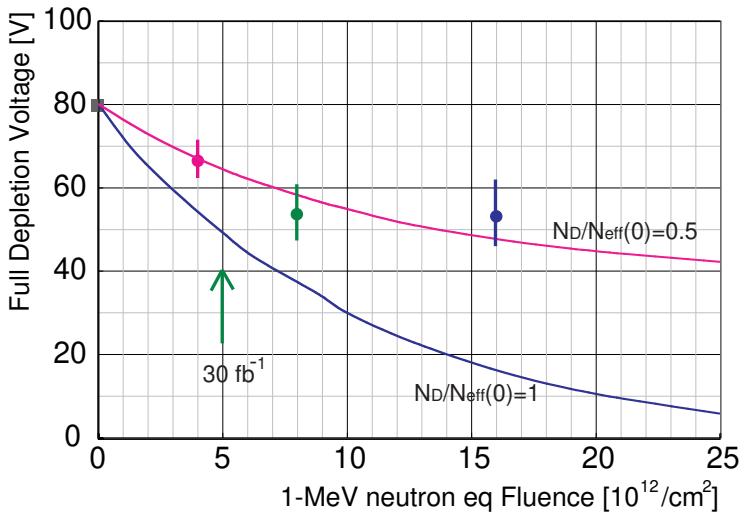

Fig. 13. Full depletion voltages of proton irradiated sensors.

5 Summary

The production of ISL Hamamatsu sensors has completed. Among the delivery of 494 sensors, 92 sensors are Class B of which the leakage current specification was loosened. We have investigated possible instability of such sensors through long-term stability of the leakage current and the radiation hardness against γ's and protons. We have seen no notable degradation specific to Class B sensors. Both Class A and B sensors should be operational with the full depletion voltage continously decreasing in the next Tevatron RUN periods.

References

[1] A. Affolder et al., Nucl. Instrum. and Methods A 435 (1999) 44.

[2] K. Hara et al., CDF note 4893, "First batches of ISL Hamamatsu Si sensors", Feb. 1999.

[3] M. Shimojima, talk given at 7th International Conference on Instruments for Collider Beam Physics (INSTR99), Hamamatsu Japan, Nov.15–19, 1999.

[4] J. A. J. Matthews et al., CDF note 3408, "Bulk radiation damage in silicon detectors and implications for SVX II", Nov. 1995; J. A. J. Matthews et al., Nucl. Instrum. and Methods A 381 (1996) 338.

[5] K. Hara et al., Nucl. Instrum. and Methods 435 (1999) 437.

[6] G. Lindstrom et al., Nucl. Instrum. and Methds A426 (1999) 1; The quoted damage constant is 4.0×10^{-17} A/cm.

[7] A. Chilingarov et al., Nucl. Instrum. and Methds A360 (1995) 432.